ISSN 1330–0008
CODEN FIZAE4

MODIFIED TWO-DIMENSIONAL ANALYTICAL MODEL FOR CURRENT-VOLTAGE AND BREAKDOWN VOLTAGE CHARACTERISTICS OF GaAs MESFET PLANAR STRUCTURE

RIFAT RAMOVIĆ[a] and ROBERT ANDRIN[b]

[a] *Faculty of Electrical Engineering, Bulevar Revolucije 73, 11120 Belgrade, Yugoslavia*
E-mail: ramovic@kiklop.etf.bg.ac.yu

[b] *"Telekom Srbija" a.d., Department of Mobile Communications, Takovska 2, 11000 Belgrade, Yugoslavia*

Received 5 January 1998;
Accepted 30 September 1998

We present an analytical approach for modelling the planar structure of GaAs MESFET's with the aim to determine current-voltage characteristics and breakdown voltage for reverse gate-drain bias. With the two-dimensional analytic solutions, we can determine the electric potential and field, and carrier and velocity profiles in the device. The results of simulation are compared with the available experimental data.

PACS numbers: 72.20.-i, 85.30.Tv UDC 537.311, 537.539

Keywords: planar MESFET structure, two-dimensional solution, electric potential and field, current-voltage characteristics, breakdown voltage

1. Introduction

The demands for optimization of various GaAs semiconductor devices require improved models of their behaviour [1–9]. Analytical models are suitable because they can include many effects with no need for previous experimental measurement which is convenient for designing new and modifying the existing devices.

A number of papers deal with the analytical behaviour of GaAs MESFETs [1–3,6,7]. Taking into consideration their results, we present modified two-dimensional models for the planar structure. In our models, we take the effect of surface states which was not the case in previous models [1–3,6], and determine the analytical solution of the two-dimensional Poisson equation. We derive relations for the potential distribution, the field distribution and carrier profiles in the channel that allows the calculation of the *I-V* characteristics and the breakdown voltage for reverse gate-drain bias, the carrier velocity distribution and the concentration of the carriers.

The reverse breakdown voltage is a significant factor limiting the microwave power output of GaAs MESFETs. There are certain effects that should be described [6,7,10–13] and better design solutions should be sought for. We found that certain effects (surface states, insulation materials) can be described with our model.

2. The model

Schematic diagram of the analyzed planar MESFET structure is given in Figs. 1 and 2. To simplify the analysis, we divide the channel into four regions, along the longitudinal axis. In comparison with previous models, the region IV is new in the analysis, where we take into account the effect of surface states.

Figure 1 shows the region I (under the gate), where the strength of electric field is below E_T (the threshold field at which the electron drift velocity attains the

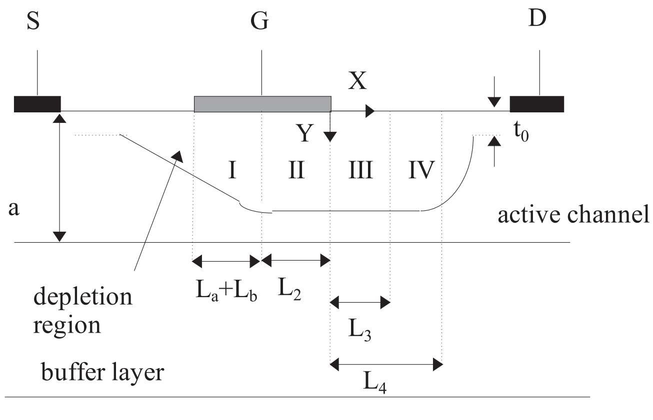

Fig. 1. Schematic diagram (cross-section) of a planar MESFET structure for the analysis of I-V characteristics.

maximum value) and this is the low-field region. The values L_a and L_b are determined as in Ref. 1. In the region II (also under the gate), the electric field is stronger than E_T. That is the case in regions III and IV, but they are not under the gate. In the region IV we introduce the effects of surface states.

Based on the analysis in Ref. 1, we assume the constant channel cross-section in the regions II, III and IV. The region IV is new in comparison with the models given in the literature, and in this region we consider the effects of the surface states.

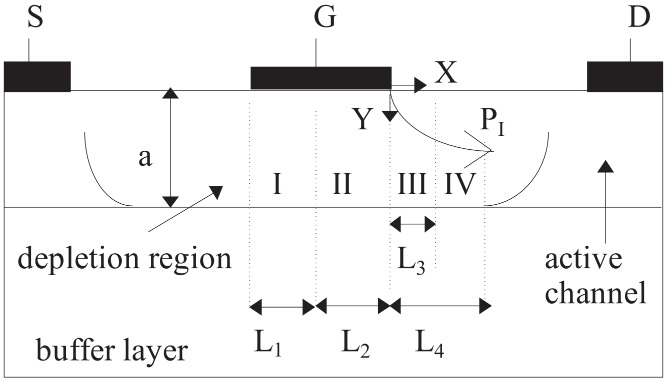

Fig. 2. Schematic diagram (cross-section) of a planar MESFET structure for the analysis of breakdown voltage characteristics.

For the analysis of the breakdown region, we use Fig. 2. Regions I and II are symmetric with respect to the center of the gate electrode [6]. In the analysis, we assume the source and drain electrodes grounded.

To get the potential distribution as a function of the parameters relevant for the analysis of the given structure for all regions of the channel, it is necessary to solve the two-dimensional Poisson equation:

$$\frac{\partial^2 V}{\partial X^2} + \frac{\partial^2 V}{\partial Y^2} = -\frac{q\, N_D(Y)}{\varepsilon_s}. \tag{1}$$

The boundaries of the regions are determined by boundary conditions [1,2,6]. As the boundary conditions, we assume the continuity of the potential across the interface, and that the transverse electric field vanishes at the boundary of the depleted region. Then, we assume that the electric field along the channel is continuous at the boundary of the depleted region [1,6].

The boundary conditions for region IV, that accounts for surface states are

$$\frac{\partial V_{IV}}{\partial Y}\,(L_3, 0) = \gamma\, \frac{\rho_{ss}}{\varepsilon_s} \tag{2}$$

$$\frac{\partial V_{IV}}{\partial Y}\,(L_4, 0) = \vartheta\, \frac{\rho_{ss}}{\varepsilon_s} \tag{3}$$

where ϑ and γ are parameters where: $\vartheta < \gamma, \gamma > 1, \vartheta = 1$. These conditions are due to the assumptions that the amount of the surface states becomes smaller at a larger distance from the gate edge. Then the universal solution of the Poisson equation has the form [1,6]:

$$V(x,y) = [A\exp(kx) + B\exp(-kx)] \times [C\cos(ky) + D\sin(ky)] + F(x^3 - 3xy^2)$$
$$+G(y^3 - 3x^2y) + H(x^2 - y^2) + Ixy + Jx + Ky + M - \frac{q}{\varepsilon_s}\int_0^y \mathrm{d}y' \int_0^{y'} N_D(y'')\mathrm{d}y'' \tag{4}$$

where A,B,C,D,E,F,G,H,I,J,K,M and k are constants which are to be determined.

The drain current is determined as

$$I_D = I_c + V_D/R_P \tag{5}$$

where I_c is the channel current calculated as

$$I_c = qZ\frac{\mathrm{d}V}{\mathrm{d}x} \int_h^a N_D(y)\,\mu(y)\,\mathrm{d}y \tag{6}$$

in the linear region and

$$I_c = qZ\int_h^a N_D(y)\,\mu(y)\,\mathrm{d}y \,\frac{E}{\sqrt{1+\left(\frac{E-E_L}{E_c}\right)^2}} \tag{7}$$

in the knee region. V_D is the drain voltage, R_P the substrate resistance, Z the channel width, V the potential, h the depletion width, a the active channel depth, E the electric field, E_c and E_L are the constants determined in Ref. 1, N_D the doping concentration and ρ_{ss} is the surface charge. In the saturation region the channel current becomes constant.

The breakdown voltage can be determined using the relation [6]

$$\int_{P_I} \alpha_n \exp\left(-\int_o^s (\alpha_n - \alpha_p)\mathrm{d}s'\right)\mathrm{d}s = 1 \tag{8}$$

where α_n is the electron ionization rate, α_p the hole ionization rate, P_I the integral path along the streamline of the electric field emanating from the gate edge and s the path length. Ionization coefficients are determined from the relations

$$\alpha_n = 2.994\times 10^5 \exp\left[-\left(\frac{6.848\times 10^5}{E}\right)^{1.6}\right] \tag{9}$$

$$\alpha_p = 2.215\times 10^5 \exp\left[-\left(\frac{6.570\times 10^5}{E}\right)^{1.75}\right] \tag{10}$$

where α_n and α_p are given in cm^{-1}.

The solutions for the potential distribution in region IV for the current-voltage characteristics are given in Eq. (11), and for the breakdown voltage in Eq. (14).

$$V_{IV,I\text{–}V}(X,Y) = \frac{2E_T h_T}{\pi}\sinh\left(\frac{\pi L_2}{2h_T}\right)\exp\left(-\frac{\pi X}{2h_T}\right)\sin\left(\frac{\pi Y}{2h_T}\right)$$

$$+\left(X^3-3XY^2\right)\frac{\alpha_2}{6h_T\left(L_4-L_3\right)}+\left(X^2-Y^2\right)\left[\frac{-L_2\alpha_2}{2h_T\left(L_4-L_3\right)}-\frac{L_3\alpha_1}{h_T^2}\right]$$

$$+XY\frac{\alpha_2}{\left(L_4-L_3\right)}+X\cdot\left[\frac{2L_3L_4}{h_T^2}\alpha_1-\frac{\alpha_2}{2h_T\left(L_4-L_3\right)}\left[2L_3L_4-L_4^2-h_T^2\right]+E_T\right]$$

$$+Y\cdot\left[E_D-\frac{L_3\alpha_2}{\left(L_4-L_3\right)}-\frac{2L_3\alpha_1}{h_T}\right]+\frac{2E_Th_T}{\pi}\sinh\left(\frac{\pi L_2}{2h_T}\right)\left[1-\exp\left(-\frac{\pi L_4}{2h_T}\right)\right]$$

$$+V_D-I_cR_D+\frac{q}{\varepsilon_s}\int_0^{h_T}\mathrm{d}Y\int_0^{Y}N_D(Y')\mathrm{d}Y'+\frac{L_3\alpha_1}{h_T^2}\left(h_T^2-L_4^2\right)-E_TL_4-E_Dh_T$$

$$+\frac{1}{L_4-L_3}\left(\alpha_2h_T\left(L_3-L_4\right)+\frac{\alpha_2}{2h_T}\left(L_3\left(L_4^2-h_T^2\right)+L_4\left(\frac{2L_4^2}{3}-2L_3L_4+2h_T^2\right)\right)\right)$$

$$+Vo-\frac{q}{\varepsilon_s}\int_0^{Y}\mathrm{d}Y'\int_0^{Y'}N_D(Y'')\mathrm{d}Y'', \tag{11}$$

where

$$\alpha_1 = E_{D,I\text{–}V}+E_{FC}-E_T\cosh\left(\frac{\pi L_2}{2h_T}\right) \tag{12}$$

$$\alpha_2 = \vartheta\frac{\rho_{ss}}{\varepsilon_s}+\frac{2L_3}{h_T}\alpha_1-E_D-E_T\sinh\left(\frac{\pi L_2}{2h_T}\right)\exp\left(-\frac{\pi L_4}{2h_T}\right) \tag{13}$$

where $E_D = (q/\varepsilon_s)\int_0^{h_T}N_D(y)\mathrm{d}y$, h_T is the depletion width in the saturated region, E_{FC} is the surface field due to the fixed charge density in the passivation insulator and $V_0 = V_G - V_{bi}$.

$$V_{IV,Vbr}(X,Y) = V_A\cosh(kL_2)\exp(-kX)\sin(kY)+$$

$$
\left(X^3-3XY^2\right)\frac{\alpha_1}{6a\left(L_4-L_3\right)}+\left(X^2-Y^2\right)\left[\frac{-L_3\alpha_1}{2a\left(L_4-L_3\right)}-\frac{L_3\alpha_2}{a^2}\right]+XY\frac{\alpha_1}{\left(L_4-L_3\right)}
$$

$$
+X\cdot\left[\frac{\left(L_3^2-a^2\right)}{a^2}\alpha_2-\left\{E_{D,Vbr}+E_{FC}+V_A\,k\cosh\left(kL_2\right)\right\}+\frac{L_3^2\,\alpha_1}{a\left(L_4-L_3\right)}\right]
$$

$$
+Y\cdot\left[E_{D,Vbr}-\frac{L_3\,\alpha_1}{\left(L_4-L_3\right)}-\frac{2L_3\,\alpha_2}{a}\right]+\alpha_2\left[L_3-\frac{L_3^3}{3a^2}\right]-\frac{2}{3}\,\frac{L_3^3}{a^2}\,\frac{\alpha_1}{\left(L_4-L_3\right)}
$$

$$
+Vo-\frac{q}{\varepsilon_s}\int\limits_0^Y\mathrm{d}y\int\limits_0^y N_D(y')\mathrm{d}y', \tag{14}
$$

where $k=\pi/2a$, $E_{D,Vbr}=(q/\varepsilon_s)\int_0^a N_D(y)\mathrm{d}y$, and

$$
V_A=\frac{\gamma(\rho_{ss}/\varepsilon_s)-E_{D,Vbr}+(2L_3/a)\;\left(E_{D,Vbr}+E_{FC}\right)}{k\cdot\left[\cosh\left(kL_2\right)\exp\left(-kL_3\right)+(2L_3/a)\;\sinh\left(kL_2\right)\right]}, \tag{15}
$$

$$
\alpha_1=\gamma\frac{\rho_{ss}}{\varepsilon_s}-E_{D,Vbr}+\frac{2L_3}{a}\alpha_2-k\,V_A\;\cosh\left(kL_2\right)\exp\left(-kL_4\right), \tag{16}
$$

$$
\alpha_2=E_{D,Vbr}+E_{FC}-V_A\,k\sinh\left(kL_2\right). \tag{17}
$$

Taking the derivatives of potential distributions, it is possible to calculate the electric field. The electron density along the channel can be estimated from the relation

$$
n\left(Y\right)=N_D\left(Y\right)+\frac{\varepsilon_s}{q}\;\frac{\partial^2 V}{\partial X^2}\bigg|_{Y=h_T}. \tag{18}
$$

3. *Results and discussion*

According to the presented model, we developed the algorithm for the numerical calculation of the electric field, the electron concentration in the structure and the current-voltage characteristics. We analyzed the influence of some technological and geometrical parameters on transient characteristics. Some results are presented in Figs. 3–9.

In the *I-V* characteristics simulations, we calculated the influence of the short channel on the threshold voltage. Results of simulation show that when the gate-source voltage is closer to the threshold voltage, the drain currents have smaller

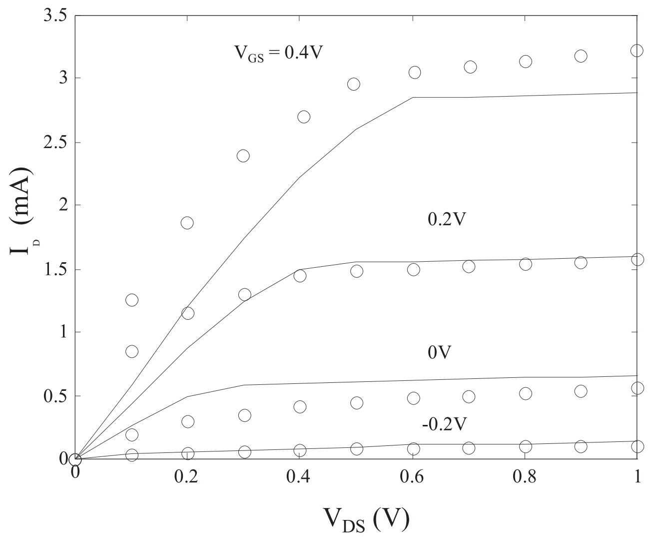

Fig. 3. I-V characteristics of GaAs *MESFET. Experimental results from Ref. 6 are marked by circles. Device parameters are:* $a = 0.12\,\mu$m, $Z = 100\,\mu$m, $N_D = 1.0\times10^{17}$cm^{-3}, $L = 2.0\,\mu$m.

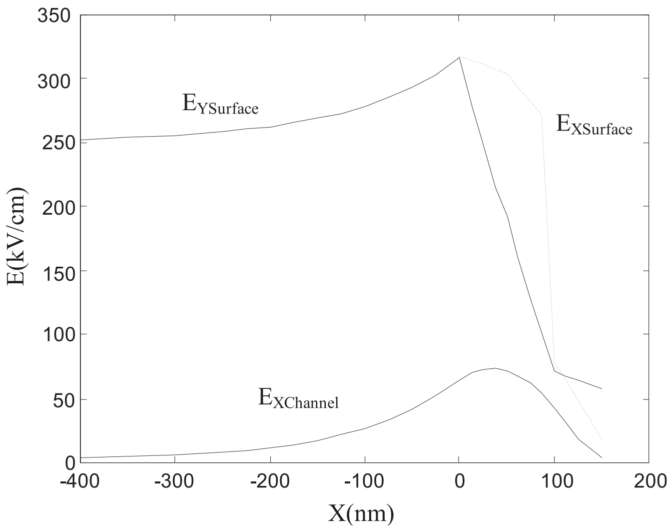

Fig. 4. The calculated electric field.

values because the active channel becomes narrower. For the high-field region, maximum field at the surface is on the drain side of the gate electrode. In the channel, the maximum value is between these two electrodes. The electric field de-

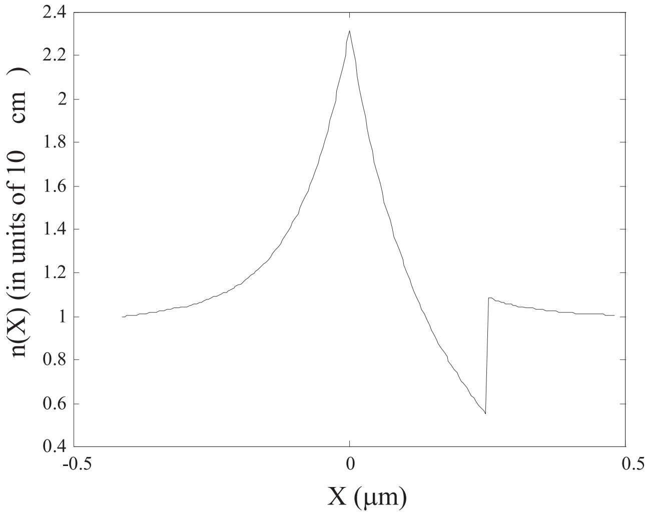

Fig. 5. The calculated electron concentration of GaAs *MESFET device.*

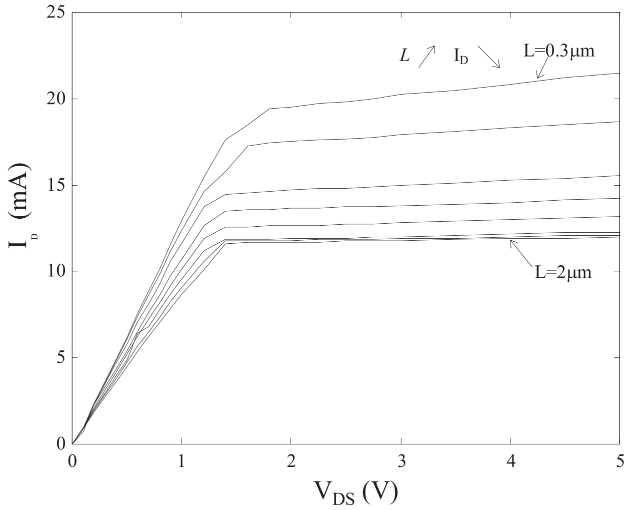

Fig. 6. The calculated I-V characteristic of GaAs *MESFET device for different gate lengths. Simulation parameters are:* $a = 0.2$ μm, $Z = 100$ μm, $N_D = 1.0 \times 10^{17}$ cm^{-3}, $V_{GS} = 0$ V. *Gate lengths are:* 0.3 μm, 0.5 μm, 0.7 μm, 1.25 μm, 1.5 μm, 1.75 μm and 2.0 μm.

cays very quickly from the gate electrode. *I-V* characteristics for the different gate lengths show that the differences become smaller for the greater gate-length values and are not like those in classical relations. For smaller gate lengths the differences are bigger.

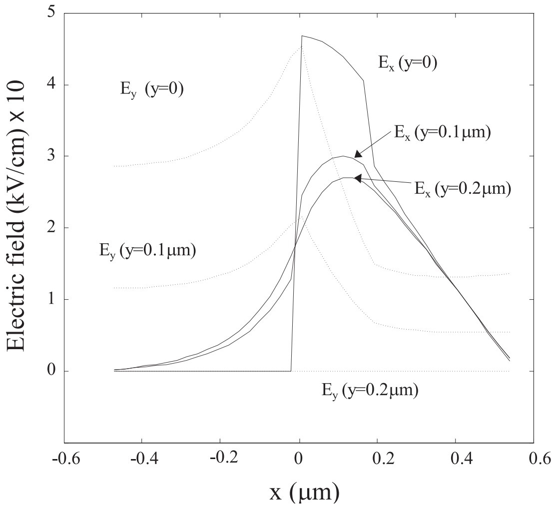

Fig. 7. The calculated electric field. Transversal fields are shown by "- - ". Device parameters are: $a = 0.2\,\mu$m, $L_G = 1\,\mu$m, $N_D = 1.0 \times 10^{17}$ cm^{-3}.

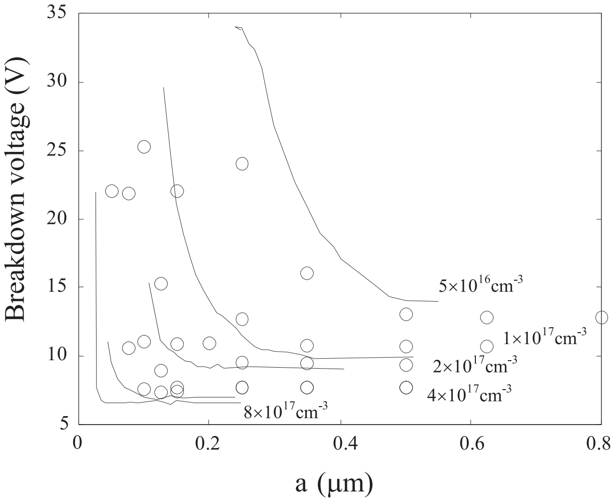

Fig. 8. Simulated results for breakdown voltages as a function of active channel depth with doping concentration as a parameter. Experimental results after Ref. 1 are marked with circles.

Simulated results for the breakdown voltages are shown in Figs. 7–9. Figure 8 shows a good agreement with the experimental results. The breakdown voltages depend much on the technological and geometrical parameters, like doping concentration and active channel thickness. The influence of the electric field strength is greater near the surface. So with a greater channel thickness, the breakdown voltages become constant, because electric fields at greater distances are negligible in comparison with the values near the surface.

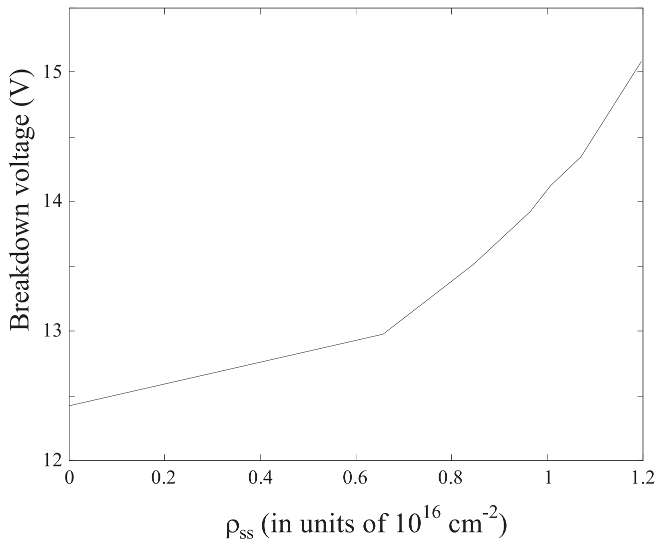

Fig. 9. The breakdown voltage as a function of the density of surface states. Device parameters are: $a = 0.2\,\mu$m, $L_G = 1\,\mu$m, $N_D = 1.0 \times 10^{17}$ cm^{-3}.

The relations among the breakdown voltages are not proportional to the doping concentration according to the relations (8–10). We can see that the electric fields attain maximum values near the edge of gate electrode and the aim of designers is to have these fields small [11–13]. The influence of the surface states is not negligible (Fig. 9) and is in accordance with the results of Ref. 10. The results can also be used and for the overlapping-gate structure [12].

4. Conclusion

We presented an analytical model of GaAs MESFET. The model is suitable for simulations because all parameters for the analysis are described by analytical expressions. This simplifies the analysis and allows predicting of the device behaviour and adjustment of technological parameters to the device project demands, thus decreasing the costs of designing of new devices. The parameters incorporated in the serial resistance models deliver results in agreement with SPICE models that the new simulators commonly use.

In the model for *I-V* characteristic, we solved analytically the two-dimensional Poisson equation that allows the analysis of electric fields inside the channel and prediction of the device behaviour in the cases of high voltage and/or high fields, which is of great importance in the design of new and for modifying the existing devices.

References

1) C.-S. Chang and D.-Y. Day, IEEE Trans. Electron Devices **2** (1989) 269;
2) R. Andrin and R. Ramović, Nauka, Tehnika, Bezbednost (Belgrade) **1** (1996) 11;
3) M. A. Khatibzadeh, R.J. Trew, IEEE Trans. Microwave Theory Tech. **2** (1988) 231;
4) M. J. Hurt, M. S. Shur, W. C. B. Peatman and P. B. Rabkin, IEEE Trans. Electron Devices **2** (1996) 358;
5) T. Ytterdal, B. Y. Moon, T.A. Fjeldly and M. Shur, IEEE Trans. Electron Devices **10** (1995) 1724;
6) C.-S. Chang and D.-Y.S. Day, Solid-State Electronics **11** (1988) 971;
7) Y.Wada and M. Tomizawa, IEEE Trans. Electron Devices **11** (1988) 1765;
8) K. Horio, H. Yanai and T. Ikoma, IEEE Trans. Electron Devices **11** (1988) 1778;
9) K. Horio, Y. Fuseya, H. Kusuki and H. Yanai, IEEE Trans. Microwave Theory and Tech. **9** (1989) 1371;
10) H. Mizuta, K. Yamaguchi and S. Takahashi, IEEE Trans. Electron Devices **10** (1987) 2027;
11) C. Gaquiere, B. Bonte, D. Théron, Y. Crosnier, P. Arsène-Henri and T. Pacou, IEEE Trans. Electron Devices **2** (1995) 209;
12) C. L. Chen, IEEE Trans. Electron Devices **4** (1996) 535;
13) M. Hirose, K. Matsuzawa, M. Mihara, T. Nitta, A. Kameyama and N. Uchitomi, IEEE Trans. Electron Devices **12** (1996) 2062;
14) M. P. Zaitlin, IEEE Trans. Electron Devices **11** (1986) 1635.

IZMIJENJENI DVODIMENZIJSKI ANALITIČKI MODELI, STRUJNO-NAPONSKE KARAKTERISTIKE I NAPON PROBOJA PLANARNOG GaAs MESFETA

Predstavljamo analitičko modeliranje planarnog GaAs MESFETa i određivanje strujno-naponske karakteristike i probojnog napona u uvjetima inverzne polarizacije vrata-odvod. Pomoću dvodimenzijskih analitičkih rješenja mogu se izračunati raspodjela polja, koncentracije nositelja naboja i raspodjela njihovih brzina. Dobiveni računski rezultati prikazuju se u dijagramima i uspoređuju s dostupnim eksperimentalnim rezultatima.